

Hyperspherical Description of the Degenerate Fermi Gas: S-wave Interactions.

Seth T. Rittenhouse¹, M. J. Cavagnero², Javier von Stecher¹, and Chris H. Greene¹

¹*Department of Physics and JILA, University of Colorado, Boulder, Colorado 80309-0440*

²*Department of Physics and Astronomy,
University of Kentucky, Lexington, Kentucky 40506-0055*

(Dated: May 12, 2018)

Abstract

We present a unique theoretical description of the physics of the spherically trapped N -atom degenerate Fermi gas (DFG) at zero temperature based on an ordinary Schrödinger equation with a microscopic, two body interaction potential. With a careful choice of coordinates and a variational wavefunction, the many body Schrödinger equation can be accurately described by a *linear*, one dimensional effective Schrödinger equation in a single collective coordinate, the rms radius of the gas. Comparisons of the energy, rms radius and peak density of ground state energy are made to those predicted by Hartree-Fock (HF). Also the lowest radial excitation frequency (the breathing mode frequency) agrees with a sum rule calculation, but deviates from a HF prediction.

I. INTRODUCTION

The realization of the degenerate fermi gas (DFG) in a dilute gas of fermionic atoms has triggered widespread interest in the nature of these systems. This achievement combined with the use of a Feshbach resonance allows for a quantum laboratory in which many quantum phenomena can be explored over a wide range of interaction strengths. This leads to a large array of complex behaviors including the discovery of highly correlated BCS-like pairing for effectively attractive interactions [1, 2, 3, 4, 5]. While these pairing phenomena are extremely interesting, we believe that the physics of a pure degenerate Fermi gas, in which the majority of atoms successively fill single particle states, is worthy of further study even in the absence of pairing. This topic is addressed in the present paper, which follows a less complete archived study of the topic.[6]

The starting point for this study is that of a hyperspherical treatment of the problem in which the gas is described by a set of $3N - 1$ angular coordinates on the surface of a $3N$ dimensional hypersphere of radius R . Here N is the number of atoms in the system. This formulation is inspired by a similar study of the Bose-Einstein condensate.[7, 8, 9] Furthermore these same coordinates have been applied to finite nuclei.[10] The formulation is a rigorous variational treatment of a many-body Hamiltonian, aside from the limitations of the assumption of pairwise, zero-range interactions. In this paper, we consider only filled energy shells of atoms. This is done for analytic and calculational simplicity, but the treatment should apply to any number of atoms in open shells with modest extensions that are discussed briefly.

The main goal of this study is to describe the motion of the gas in a *single* collective coordinate R , which describes the overall extent of the gas. The benefit of this strategy is that the behavior of the gas is reduced to a single one-dimensional *linear* Schrödinger equation with an effective hyperradial potential. The use of a real potential then lends itself to the intuitive understanding of normal Schrödinger quantum mechanics. This method also allows for the calculation of physical quantities such as the energy and rms radius of the ground state; these observables agree quantitatively with those computed using Hartree-Fock methods. The method also yields a visceral understanding of a low energy collective oscillation of the gas, i.e. a breathing mode.

Beyond the intuitive benefits of reducing the problem to an effective one-dimensional

Schrödinger equation, another motivation for developing this hyperspherical viewpoint is that it has proven effective in other contexts for describing processes involving fragmentation or collisions in few-body and many-body systems.[11, 12] Such processes would be challenging to formulate using field theory or RPA or configuration interaction viewpoints, but they emerge naturally and intuitively, once the techniques for computing the hyperspherical potential curves for such systems are adequately developed. To this end we view it as a first essential step, in the development of a more comprehensive theory, to calculate the ground-state and low-lying excited state properties within this framework. Then we can ascertain whether the hyperspherical formulation is capable of reproducing the key results of other, more conventional descriptions, which start instead from a mean-field theory perspective.

The paper is organized as follows: Section II develops the formulation that yields a hyperradial 1D effective Hamiltonian; in Section III we apply this formalism to a zero-range s-wave interaction and find the effective Hamiltonian in both the finite N and large N limits. In Sections IIIa and IIIb we examine the nature of the resulting effective potential for a wide range of interaction strengths and give comparisons with other known methods, mainly Hartree-Fock (HF); Section IIIc is a brief discussion of the simplifications that can be made in the limit where $N \rightarrow \infty$; finally in Section IV we summarize the results and discuss future avenues of study.

II. FORMULATION

The formalism is similar to that of reference [7], but we will reiterate it for clarity and to make this article self-contained. Consider a collection of N identical fermionic atoms of mass m in a spherically symmetric trap with oscillator frequency ω , distributed equally between two internal spin substates. The governing Hamiltonian is

$$H = \frac{-\hbar^2}{2m} \sum_{i=1}^N \nabla_i^2 + \frac{1}{2} m \omega^2 \sum_{i=1}^N r_i^2 + \sum_{i>j} U_{int}(\vec{r}_{ij}) \quad (2.1)$$

where $U_{int}(\vec{r})$ is an arbitrary two-body interaction potential and $\vec{r}_{ij} = \vec{r}_i - \vec{r}_j$. We ignore interaction terms involving three or more bodies. In general, the Schrödinger equation that comes from this Hamiltonian is very difficult to solve. Our goal is to simplify the system by describing its behavior in terms of a *single collective coordinate*. To achieve this

aim we transform this Hamiltonian into a set of collective hyperspherical coordinates; the hyperradius, R , of this set is given by the root mean square distance of the atoms from the center of the trap.

$$R \equiv \left(\frac{1}{N} \sum_{i=1}^N r_i^2 \right)^{1/2}. \quad (2.2)$$

So far we only have one coordinate for the system, but we need to account for all $3N$ spatial coordinates and also the spin degrees of freedom. This leaves $3N - 1$ angular coordinates left to define. We have $2N$ of the angles as the independent particle spherical polar coordinate angles $(\theta_1, \phi_1, \theta_2, \phi_2, \dots, \theta_N, \phi_N)$. The remaining $N - 1$ hyperangles are chosen by the convention used in [10], which describes correlated motions in the radial distances of the atoms from the trap center,

$$\tan \alpha_i = \frac{\sqrt{\sum_{j=1}^i r_j^2}}{r_{i+1}}, \quad (2.3)$$

$$i = 1, 2, 3, \dots, N - 1.$$

Alternatively we may write this as

$$r_n = \sqrt{N} R \cos \alpha_{n-1} \prod_{j=n}^{N-1} \sin \alpha_j \quad (2.4)$$

$$0 \leq \alpha_j \leq \frac{\pi}{2}, \quad j = 1, 2, \dots, N - 1$$

where we define $\cos \alpha_0 \equiv 1$ and $\prod_{j=N}^{N-1} \sin \alpha_j \equiv 1$. For the purposes of this study, the set of $3N - 1$ hyperangles will be referred to collectively as Ω . The particular definition of the hyperangles will not play a significant role in the actual formalism, but we give the definitions here for completeness.

After carrying out this coordinate transformation on the sum of Laplacians, the kinetic energy becomes [13]

$$\frac{-\hbar^2}{2M} \left[\frac{1}{R^{3N-1}} \frac{\partial}{\partial R} \left(R^{3N-1} \frac{\partial}{\partial R} \right) - \frac{\mathbf{\Lambda}^2}{R^2} \right]. \quad (2.5)$$

Here $M = Nm$ and $\hbar\mathbf{\Lambda}$ is the grand angular momentum operator which is similar to the conventional angular momentum operator and is defined by

$$\mathbf{\Lambda}^2 = - \sum_{i>j} \Lambda_{ij}^2, \quad \Lambda_{ij} = x_i \frac{\partial}{\partial x_j} - x_j \frac{\partial}{\partial x_i} \quad (2.6)$$

for all cartesian components, x_i , of the $3N$ dimensional space. The isotropic spherical oscillator potential becomes simply

$$\frac{1}{2}m\omega^2 \sum_{i=1}^N r_i^2 = \frac{1}{2}M\omega^2 R^2. \quad (2.7)$$

The sum of Eqs. 2.5 and 2.7 gives a time-independent Schrödinger equation, $H\Psi(R, \Omega) = E\Psi(R, \Omega)$, of the form

$$0 = \left[\frac{-\hbar^2}{2M} \left(\frac{\partial^2}{\partial R^2} + \frac{(3N-1)(3N-3)}{2R^2} - \frac{\Lambda^2}{R^2} \right) + \frac{1}{2}M\omega^2 R^2 \right. \\ \left. + \sum_{i>j} U_{int}(\vec{r}_i - \vec{r}_j) - E \right] R^{(3N-1)/2} \Psi(R, \Omega) \quad (2.8)$$

where $\Psi(R, \Omega)$ has been multiplied by $R^{(3N-1)/2}$ to remove first derivative terms in the hyperradius. These mathematical transformations have not yet accomplished much. We started with a $3N$ dimensional Schrödinger equation to solve, and we still have a $3N$ dimensional Schrödinger equation. To simplify, we assume that Ψ is approximately separable into an eigenfunction of the operator Λ^2 , a ‘‘hyperspherical harmonic’’, multiplied by an unknown hyperradial function. Hyperspherical harmonics (HHs, see [13] for more details) are generally expressed as products of Jacobi polynomials for any number of dimensions. Their eigenvalue equation is

$$\Lambda^2 \Phi_{\lambda\nu}(\Omega) = \lambda(+\lambda + 3N - 1) \Phi_{\lambda\nu}(\Omega) \quad (2.9)$$

Where $\lambda = 0, 1, 2, \dots$ and ν (omitted below for brevity) stands for the $3N - 2$ other quantum numbers that are needed to distinguish between the (usually quite large) degeneracies for a given λ . The separability ansatz implies that

$$\Psi(R, \Omega) = F(R) \Phi_{\lambda}(\Omega). \quad (2.10)$$

Here we assume that $\Phi_{\lambda}(\Omega)$ is the HH that corresponds to the lowest value of the hyperangular momentum that is allowed for the given symmetry of the problem, i.e. that is antisymmetric with respect to interchange of indistinguishable fermions. This choice of trial wavefunction indicates that we expect the overall energetics of the gas to be described by its size; as such, fixing the hyperangular behavior is equivalent with fixing the configuration of the atoms in the gas. In nuclear physics this is known as the K harmonic method. Alternatively, this may be viewed as choosing a trial wavefunction whose hyperradial behavior will

be variationally optimized, but whose hyperangular behavior is that of a non-interacting trap dominated gas of fermions.

To utilize this as a trial wavefunction, we evaluate the expectation value $\langle \Phi_\lambda | H | \Phi_\lambda \rangle$, where the integration is taken over all hyperangles at a fixed hyperradius. This approach gives a new effective linear 1D Schrödinger equation $H_{eff} R^{(3N-1)/2} F(R) = E R^{(3N-1)/2} F(R)$ in terms of an effective Hamiltonian H_{eff} given by

$$\frac{-\hbar^2}{2M} \left(\frac{d^2}{dR^2} - \frac{K(K+1)}{R^2} \right) + \frac{1}{2} M \omega^2 R^2 + \sum_{i>j} \langle \Phi_\lambda | U_{int}(\vec{r}_{ij}) | \Phi_\lambda \rangle. \quad (2.11)$$

Here $K = \lambda + 3(N-1)/2$.

We now must force our trial wavefunction to obey the antisymmetry condition of fermionic atoms. To antisymmetrize the total wave function $F(R) \Phi_\lambda(\Omega)$ note that Eq. 2.2 indicates that R is completely symmetric under all particle coordinate exchange, thus the antisymmetrization of the wavefunction must only affect $\Phi_\lambda(\Omega)$. Finding a completely antisymmetric $\Phi_\lambda(\Omega)$ for any given λ is generally quite difficult and is often done using recursive techniques like coefficient of fractional parentage expansions (see [10, 14, 15] for more details) or using a basis of Slater determinants of independent particle wave functions.[16, 17, 18, 19] We use a simplified version of the second method combined with the following theorem, proved in reference [15] and developed in Appendix B.

Theorem 1 *The ground state of any non-interacting set of N particles in an isotropic oscillator is an eigenfunction of Λ^2 with minimal eigenvalue $\lambda(\lambda + 3N - 2)$ where λ is given by the total number of oscillator quanta in the non-interacting system.*

$$\lambda = \frac{E_{NI}}{\hbar\omega} - \frac{3N}{2} \quad (2.12)$$

where E_{NI} is the total ground state energy of the non-interacting N -body system.

With Theorem 1 in hand we may find $\Phi_\lambda(\Omega)$ in terms of the independent particle coordinates. The non-interacting ground state is given by a Slater determinant of single particle solutions.

$$\Psi_{NI}(\vec{r}_1, \vec{r}_2, \dots, \vec{r}_N, \sigma_1, \sigma_2, \dots, \sigma_N) = \sum_P (-1)^P P \prod_{i=1}^N R_{n_i \ell_i}(r_i) y_{\ell_i m_i}(\omega_i) |m_{s_i}\rangle. \quad (2.13)$$

Here σ_i is the spin coordinate for the i th atom, $R_{n_i \ell_i}(r_i)$ is the radial solution to the independent particle harmonic oscillator for the i th particle given by $r R_{n\ell}(r) =$

$N_{n\ell} \exp(-r^2/2l^2) (r/l)^{\ell+1} L_n^{\ell+1/2} [(r/l)^2]$ where $L_n^\alpha(r)$ is an associated Laguerre polynomial with $l = \sqrt{\hbar/m\omega}$. $y_{\ell_i m_i}(\omega_i)$ is an ordinary 3D spherical harmonic with ω_i as the spatial solid angle for the i th particle, $|m_{s_i}\rangle$ is a spin ket that will allow for two spin species of atoms, $|\uparrow\rangle$ and $|\downarrow\rangle$. The sum in Eq. 2.13 runs over all possible permutations P of the N spatial and spin coordinates in the product wavefunction. We now apply Theorem 1 which directly leads to a Ψ_{NI} that is separable into a hyperangular piece and a hyperradial piece

$$\Psi_{NI}(\vec{r}_1, \vec{r}_2, \dots, \vec{r}_N, \sigma_1, \sigma_2, \dots, \sigma_N) = G(R) \Phi_\lambda(\Omega, \sigma_1, \sigma_2, \dots, \sigma_N). \quad (2.14)$$

Here $G(R)$ is the nodeless hyperradial wave function describing the ground state of N non-interacting atoms in an isotropic oscillator trap. A derivation of $G(R)$ is given in Appendix A:

$$R^{(3N-1)/2} G(R) = A_\lambda \exp(-R^2/2\mathcal{L}^2) \left(\frac{R}{\mathcal{L}}\right)^{\lambda+3N/2-1/2}, \quad (2.15)$$

here A_λ is a normalization constant and $\mathcal{L} = \sqrt{\hbar/M\omega} = l/\sqrt{N}$. Combining Eq. 2.14 with Eq. 2.15 now gives us $\Phi_\lambda(\Omega)$

$$\Phi_\lambda(\Omega, \sigma_1, \sigma_2, \dots, \sigma_N) = \frac{\sum_P (-1)^P P \prod_{i=1}^N R_{n_i \ell_i}(r_i) y_{\ell_i m_i}(\omega_i) |m_{s_i}\rangle}{G(R)} \quad (2.16)$$

where we must make the variable substitutions in the numerator using Eqs. 2.2 and 2.3. In the following, for brevity, the spin coordinates $(\sigma_1, \dots, \sigma_N)$ will be suppressed, i.e. $\Phi_\lambda(\Omega) = \Phi_\lambda(\Omega, \sigma_1, \sigma_2, \dots, \sigma_N)$. Interestingly, this must be a function only of the hyperangles and thus all of the hyperradial dependence must cancel out in the right hand side of 2.16. We are now ready to start calculating the interaction matrix element $\langle \Phi_\lambda | U_{int} | \Phi_\lambda \rangle$.

III. ZERO-RANGE S-WAVE INTERACTION.

Here we specify $U_{int}(\vec{r})$ as a zero-range two body interaction with an interaction strength given by a constant parameter g .

$$U_{int}(\vec{r}) = g\delta^3(\vec{r}) \quad (3.1)$$

For a small two body, s-wave scattering length a we know that $g = \frac{4\pi\hbar^2 a}{m}$. [20] For stronger interactions, i.e. $|k_f a| > 1$, this approximation no longer holds and g must be renormalized.

Now we must calculate the effective interaction matrix element given by

$$U_{eff}(R) = g \sum_{i>j} \langle \Phi_\lambda | \delta^3(\vec{r}_{ij}) | \Phi_\lambda \rangle. \quad (3.2)$$

Degenerate ground states cause some complications for this formulation which we avoid by restricting ourselves to the non-degenerate ground states that correspond to filled energy shells of the oscillator, i.e. “magic numbers” of particles. With moderate extensions the degeneracies can be taken into account by creating an interaction matrix, but the magic number restriction should still give a good description of the general behavior of systems with large numbers of atoms. The total number of atoms and the hyperangular momentum quantum number λ are most conveniently expressed in terms of the number n of single particle orbital energies filled:

$$N = \frac{n(n+1)(n+2)}{3} \quad (3.3a)$$

$$\lambda = \frac{(n-1)n(n+1)(n+2)}{4} \quad (3.3b)$$

$$k_f = \sqrt{\frac{2m\omega}{\hbar} \left(n + \frac{1}{2} \right)}, \quad (3.3c)$$

where k_f is the peak non-interacting Fermi wave number. In the limit where $N \gg 1$, we write λ and k_f in terms of the total number of particles N ,

$$\lambda \rightarrow \frac{(3N)^{4/3}}{4} \quad (3.4a)$$

$$k_f \rightarrow \sqrt{\frac{2m\omega}{\hbar}} (3N)^{1/3} \quad (3.4b)$$

Next we combine 3.4a with $\Phi_\lambda(\Omega)$ from 2.16 and calculate the interaction matrix element.

Since $\Phi_\lambda(\Omega)$ is antisymmetric under particle exchange we may do a coordinate transposition in the sum $\vec{r}_i \rightarrow \vec{r}_2$ and $\vec{r}_j \rightarrow \vec{r}_1$. Each transposition pulls out a negative sign from Φ_λ and we are left with

$$\begin{aligned} U_{eff}(R) &= g \sum_{i>j} \langle \Phi_\lambda | \delta^3(\vec{r}_{21}) | \Phi_\lambda \rangle \\ &= g \frac{N(N-1)}{2} \langle \Phi_\lambda | \delta^3(\vec{r}_{21}) | \Phi_\lambda \rangle. \end{aligned}$$

Appendix C details the calculation of the matrix element $\langle \Phi_\lambda | \delta^3(\vec{r}_{21}) | \Phi_\lambda \rangle$. The result is

$$U_{eff}(R) = g \frac{C_N}{N^{3/2} R^3} \quad (3.5)$$

where C_N is a constant that is dependent only on the number of atoms in the system. While C_N has some complex behavior for smaller numbers of particles, we have seen that for $N \gtrsim 100$, C_N quickly converges to

$$\begin{aligned} C_N &\rightarrow \sqrt{\frac{2}{3}} \frac{32N^{7/2}}{35\pi^3} \left(1 + \frac{0.049}{N^{2/3}} - \frac{0.277}{N^{4/3}} + \dots \right) \\ &= 0.02408N^{7/2} \left(1 + \frac{0.049}{N^{2/3}} - \frac{0.277}{N^{4/3}} + \dots \right) \end{aligned} \quad (3.6)$$

where the higher order terms in $1/N$ were found by fitting a curve to numerically calculated data. Values of $C_N/N^{7/2}$ versus $1/N$ are shown in Fig. 1 shows both the

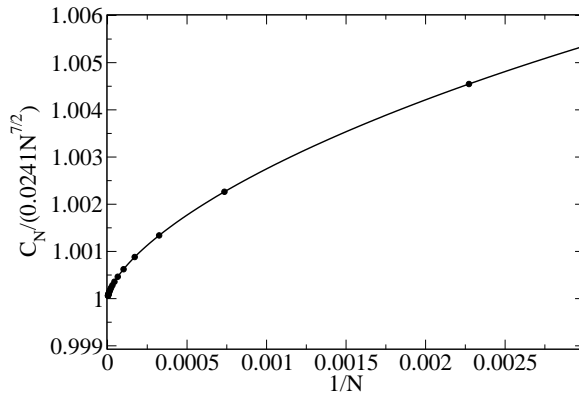


FIG. 1: Values of C_N divided by the large N limit, $C_N \rightarrow 0.02408N^{7/2}$, versus $1/N$ are shown. The circles are the calculated value while the curve is the fit stated in Eq. 3.6

calculated values of C_N and the values from the fit in Eq. 3.6 versus $1/N$. In both the table and the plot we can clearly see the convergence to the large N value of $C_N \approx 0.02408N^{7/2}$.

We now may write the effective one dimensional, hyperradial Schrödinger equation, $H_{eff}R^{(3N-1)/2}F(R) = ER^{(3N-1)/2}F(R)$ where H_{eff} is given by

$$H_{eff} = -\frac{\hbar^2}{2M} \frac{d^2}{dR^2} + V_{eff}(R) \quad (3.7)$$

where $V_{eff}(R)$ is an effective hyperradial potential given by

$$V_{eff}(R) = \frac{\hbar^2}{2M} \frac{K(K+1)}{R^2} + \frac{1}{2}M\omega^2R^2 + g\frac{C_N}{N^{3/2}R^3} \quad (3.8)$$

We reinforce the idea that this effective Hamiltonian describes the fully correlated motion of all of the atoms in the trap albeit within the aforementioned approximations. As expected, for $N = 1$, with $C_1 = 0$, Eq. 3.8 reduces to a single particle in a trap with K as the angular

n	N	λ	$C_N/N^{7/2}$
1	2	0	$\frac{1}{8\pi^2} \approx 0.0127$
2	8	6	0.0637
3	20	30	0.0251
4	40	90	0.0244
5	70	210	0.02435
...
15	1360	14280	0.0241
30	9920	215760	0.02409
100	343400	25497450	0.02408

TABLE I: N , λ and $C_N/N^{7/2}$ for the several filled shells. We can see that $C_N/N^{7/2}$ quickly converges to the Thomas-Fermi limiting value of $32\sqrt{2/3}/35\pi^3 \approx 0.02408$ to several digits.

momentum quantum number ℓ . Note that the form of V_{eff} is very similar to the effective potential found for bosons by the authors of [7]. What may be surprising is the extra term of $3(N-1)/2$ contained in K . The kinetic energy term in V_{eff} is controlled by the hyperangular momentum, which in turn reflects the total nodal structure of the N -fermion wavefunction. This added piece of hyperangular momentum summarizes the energy cost of confining N fermions in the trap. This repulsive barrier stabilizes the gas against collapse for attractive interactions, i.e. $g < 0$.

A final transformation simplifies the radial Schrödinger equation, namely setting $E = E_{NI}E'$ and $R = \sqrt{\langle R^2 \rangle_{NI}}R'$ where

$$E_{NI} = \hbar\omega \left(\lambda + \frac{3N}{2} \right), \quad (3.9a)$$

$$\langle R^2 \rangle_{NI} = l^2 \left(\frac{\lambda}{N} + \frac{3}{2} \right) \quad (3.9b)$$

are the non-interacting expectation values of the energy and squared hyperradius in the ground state. In the following any hyperradius with a prime, R' denotes the hyperradius in units of $\sqrt{\langle R^2 \rangle_{NI}}$. Under this transformation, with the use of Eqs. 3.4a and 3.4b, and in the limit where $N \rightarrow \infty$, the hyperradial Schrödinger equation becomes

$$\left(\frac{-1}{2m^*} \frac{d^2}{dR'^2} + \frac{V_{eff}(R')}{E_{NI}} - E' \right) R'^{(3N-1)/2} F(R') = 0 \quad (3.10)$$

where $m^* = (\lambda + 3N/2)^2$. The effective potential takes on the simple form

$$\frac{V_{eff}(R')}{E_{NI}} \rightarrow \frac{1}{2R'^2} + \frac{1}{2}R'^2 + \frac{\sigma k_f \gamma}{R'^3}. \quad (3.11)$$

where $\sigma = 1024/2835\pi^3$ and $\gamma = g/\hbar\omega l^2$. We note that the only parameter that remains in this potential is the dimensionless quantity $k_f \gamma$ and that in oscillator units $\gamma = g$.

In the limit where $N \rightarrow \infty$ the effective mass m^* becomes

$$m^* \rightarrow \frac{1}{16} (3N)^{8/3}. \quad (3.12)$$

For large numbers of particles, the second derivative terms in Eq. 3.10 becomes negligible, a fact used later in Section IIIc.

The behavior of $V_{eff}(R')$ versus R' is illustrated in Fig. 2 for various values of $k_f \gamma$. For

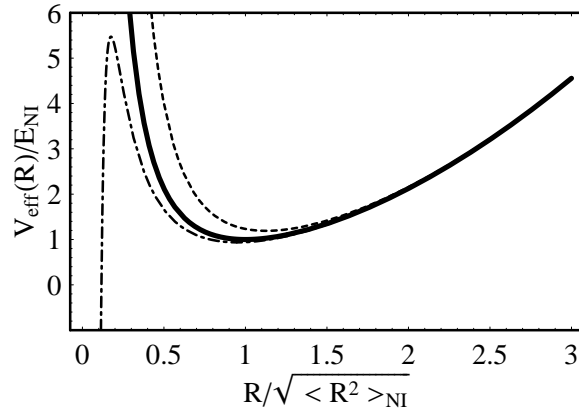


FIG. 2: The effective potential as a function of the hyperradius for $k_f \gamma = 0$ (solid), $k_f \gamma = 15$ (dashed) and $k_f \gamma = -5$. (dot-dash)

$k_f \gamma = 0$ (solid curve), the non-interacting limit, the curve is exact and the ground state solution is given by equation 2.15. For non-zero values of g , V_{eff} acquires an attractive ($k_f \gamma < 0$) or repulsive ($k_f \gamma > 0$) $1/R^3$ contribution as indicated by the dot-dashed and dashed lines respectively. For $k_f \gamma < 0$ the DFG is metastable in a region which has a repulsive barrier which it may tunnel through and emerges in the region of small R' where the interaction term is dominant. It should be noted, though, that small R' means the overall size of the gas is small. Thus the region of collapse corresponds to a very high density in the gas. In this region several of the assumptions made can fall apart, most notably the assumption dealing with the validity of the two-body, zero-range potential.[21] For $k_f \gamma > 0$ the positive $1/R^3$ serves to strengthen the repulsive barrier and pushes the gas further out.

A. Repulsive interactions ($g > 0$)

For positive values of the interaction parameter g we expect the predicted energy for this K harmonic method to deviate from experimental values, since the trial wavefunction does not allow any fermions to combine into molecular pairs as has been seen in experiments.[1, 2, 4, 5] Our method only can describe the normal degenerate fermi gas. The strong repulsive barrier for repulsive interactions shown in Fig. 2 arises as the gas pushes against itself which increases the

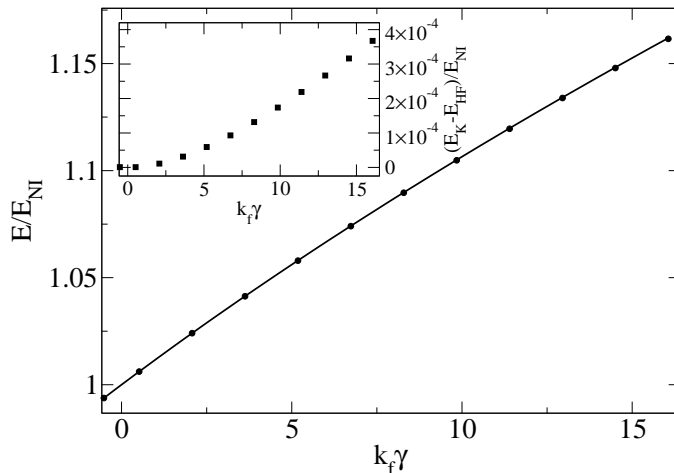


FIG. 3: The ground state energy in units of the non-interacting energy versus $k_f \gamma$ for 240 atoms calculated using the K harmonic method (curve) and using Hartree-Fock (circles). Inset: the difference in the ground state energies predicted by the K harmonic (E_K) and Hartree-Fock (E_{HF}). Clearly the K harmonic energies are slightly higher than Hartree-Fock.

the ground state energy and average radius squared respectively of 240 trapped atoms, plotted as a function of $k_f \gamma$ with a Hartree-Fock (HF) calculation. The inset in Fig. 3 shows that the K harmonic energies are slightly above the HF energies; since both methods are variational upper bounds, we can conclude that the Hartree-Fock solution is a slightly better representation of the true solution to the full Schrödinger equation with δ -function interactions.

An added benefit of the K harmonic method is that we now have an intuitively simple way to understand the energy of the lowest radial excitation of the gas, i.e. the breathing mode frequency. Fig. 2 shows that as $k_f \gamma$ increases the repulsion increases the curvature

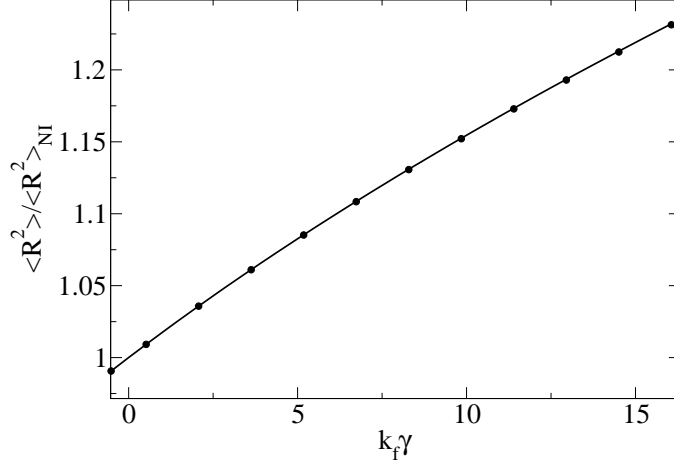


FIG. 4: The ground state average squared radius of the gas atoms in units of the non-interacting rms squared radius is plotted versus $k_f \gamma$. The calculations considered 240 atoms in both the K harmonic method (curve)

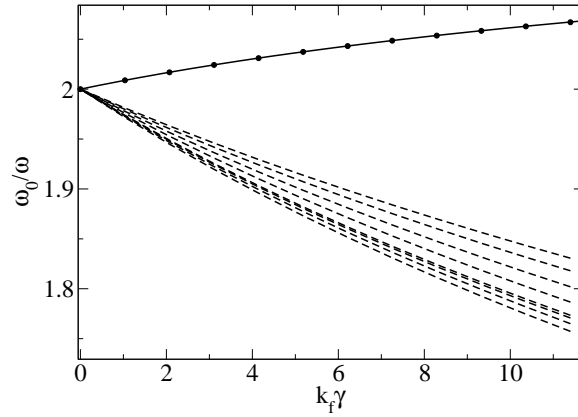


FIG. 5: The lowest breathing mode excitation (ω_0) in units of the trap frequency is plotted versus $k_f \gamma$ for the K harmonic method (solid curve) and for the sum rule (circles). Also shown as dashed curves are the lowest eight radial excitation frequencies predicted in the Hartree-Fock approximation.

at the local minimum, whereby stronger repulsion causes the breathing mode frequency to increase. Fig. 5 compares the breathing mode frequency calculated using the K harmonic method to the sum rule prediction [22] based on HF orbitals, and also the lowest eight radial excitation frequencies predicted by Hartree-Fock. As anticipated, the K harmonic method and the sum rule method agree that the breathing mode frequency will increase with added

repulsion. Interestingly both the K harmonic and sum rule methods disagree qualitatively with all eight of the lowest HF excitations. This difference is attributed to the fact that Hartree-Fock on its own can only describe *single particle* excitations while both the sum rule and the K harmonic methods describe *collective* excitations in which the entire gas oscillates coherently.

As another test of the K harmonic method we calculate the peak density of the gas. To do this we first define the density

$$\rho(\vec{r}) = \int \left(\prod_{j=1}^N d^3 r_j \right) \sum_{i=1}^N \delta^3(\vec{r}_i - \vec{r}) |\Psi|^2. \quad (3.13)$$

It can be seen that integration over \vec{r} using this definition gives $\int \rho(\vec{r}) d^3 r = N$. We recall that our separable approximation takes the form $\Psi = F(R) \Phi_\lambda(\Omega)$. Use of 3.13 and the antisymmetry of Φ_λ gives

$$\rho(0) = N \int dR R^{3N-1} |F(R)|^2 \int d\Omega \delta^3(\vec{r}_N) |\Phi_\lambda(\Omega)|^2. \quad (3.14)$$

The hyperangular integration is carried out in Appendix D. The result is

$$\frac{\rho(0)}{\rho_{NI}(0)} = \xi \int dR \frac{R^{3N-1} |F(R)|^2}{R^3}. \quad (3.15)$$

where $\rho_{NI}(0)$ is the non-interacting peak density and $\xi = \frac{l^3 \Gamma(\lambda + 3N/2)}{N^{3/2} \Gamma(\lambda + 3(N-1)/2)}$. For the n th filled energy shell the non-interacting peak density is given by

$$\rho_{NI}(0) \approx \frac{k_f^3}{6\pi^2} = \frac{1}{6\pi^2} \left[\frac{2m\omega}{\hbar} (n + 1/2) \right]^{3/2}$$

Note that the peak density is *not* given by $R^{3N-1} |F(R)|^2$ evaluated at $R = 0$, this describes the probability of all of the particles being at the center at once.

Fig. 6 compares the K harmonic and HF peak densities. Clearly the density does decrease from the non-interacting value. The two methods are in good qualitative agreement, but Hartree-Fock seems to predict a slightly lower density, presumably a manifestation of the slightly inferior K harmonic wavefunction, $F(R) \Phi_\lambda(\Omega)$.

B. Attractive interactions ($g < 0$)

In this section we examine the behavior of the gas under the influence of attractive s-wave interactions ($k_f \gamma < 0$). For attractive interactions the gas lives in a metastable region and

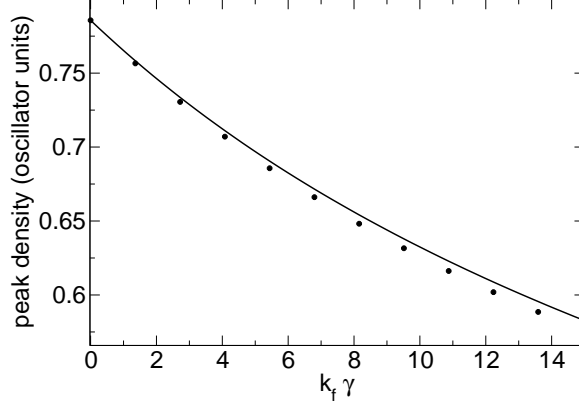


FIG. 6: The peak density in units of $(\hbar/m\omega)^{-3/2}$ versus $k_f \gamma$ predicted by the K harmonic (solid) and HF (circles). Both sets of calculations were done for a filled shell of 240 atoms.

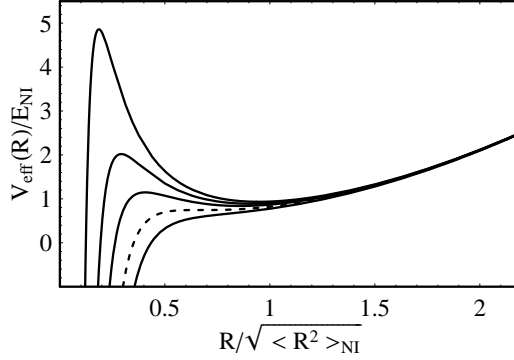


FIG. 7: V_{eff} versus R' for several values of $k_f \gamma$. $k_f \gamma = k_f \gamma_c$ (dashed) and from top to bottom $k_f \gamma = -5.3, -8.3, -11.3, -19.3$ (all solid)

can tunnel through the barrier shown in Fig. 2. Fig. 7 shows the behavior of V_{eff} for several values of $k_f \gamma$. The location of the local minimum gets pulled down with stronger attraction as the gas pulls in on itself and deeper into the center of the trap. Further, as the strength of the interaction increases, the height of the barrier decreases. In fact beyond a critical interaction strength γ_c the interaction becomes so strong that it always dominates over the repulsive kinetic term. At this critical point the local extrema disappear entirely and the gas is free to fall into the inner “collapse” region. The value of γ_c can be calculated approximately by finding the point where V_{eff} loses its local minimum and becomes entirely attractive. This is not exact as the gas will have some small zero point energy that will allow it to tunnel through or spill over the barrier before the minimum entirely disappears.

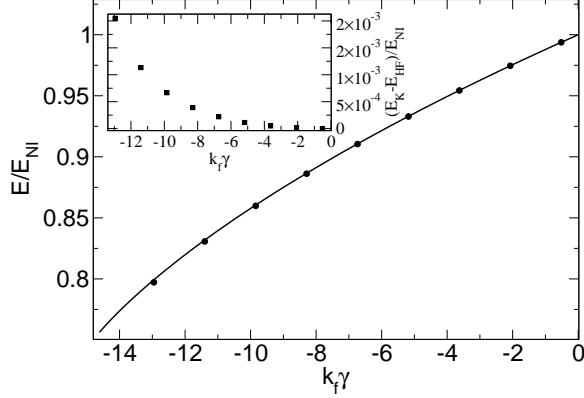


FIG. 8: The ground state energy (in units of the non-interacting energy) versus $k_f\gamma$ for 240 atoms calculated using the K harmonic (curve) and Hartree-Fock (circles) methods. Inset: The difference in the ground state energies predicted by the K harmonic (E_K) and Hartree-Fock (E_{HF}). Clearly the K harmonic prediction is slightly higher.

This critical interaction strength is given by

$$k_f\gamma_c = -\frac{189\pi^3}{256} \frac{1}{5^{1/4}} \approx -15.31.$$

Just before the minimum disappears, its location is given by $R'_{\min} = 5^{-1/4}$, with an energy of $V_{eff}(R'_{\min}) = \sqrt{5}E_{NI}/3 \approx 0.75E_{NI}$. This means that if the gas is mechanically stable for all values of the two body scattering length, i.e. $a \rightarrow -\infty$, in this approximation, there must be a renormalization cutoff in the strength of the δ -function such that $k_f\gamma > -15.31$ for all a . With this in mind, we begin to examine the behavior of the DFG for the allowed values of $k_f\gamma$.

Figs. 8 and 9 show a comparison of the ground state energy and rms radius of the gas versus $k_f\gamma$ down to the $k_f\gamma_c$ as calculated in the K harmonic and Hartree-Fock methods. Again Hartree-Fock does just slightly better in energy, which we interpret as Hartree-Fock giving a slightly better representation of the actual ground state wavefunction. The energy difference becomes largest as the interaction strength approaches the critical value. This increase is due to the fact that Hartree-Fock predicts that collapse occurs slightly earlier with $k_f\gamma_c \approx -14.1$. As the interaction strength increases, the energy and rms radius of the gas decrease. As $k_f\gamma$ approaches $k_f\gamma_c$ the overall size of the gas decreases sharply and from Eq. 3.15 we expect to see a very sharp rise in the peak density. This behavior is

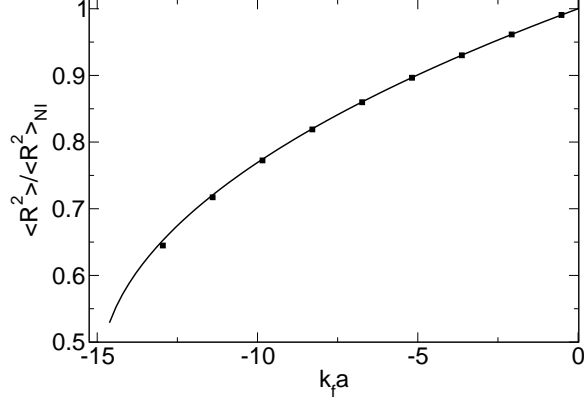


FIG. 9: The average squared radius of the Fermi gas ground state in units of the non-interacting value is plotted versus $k_f \gamma$. The calculations are for 240 atoms in both the K harmonic method (curve) and Hartree-Fock

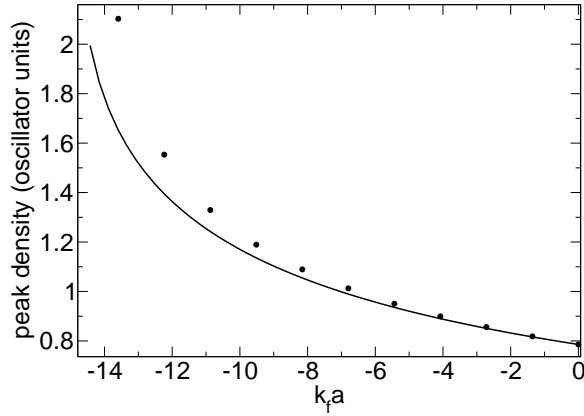


FIG. 10: The peak density in units of $(\hbar/m\omega)^{-3/2}$ versus $k_f \gamma$ predicted by the K harmonic (solid line) and HF (circles). Both calculations were carried out for a filled shell of 240 atoms.

apparent in Fig. 10, which displays the peak density versus $k_f \gamma$ for both the K harmonic and Hartree-Fock.

While the local minimum present in V_{eff} only supports metastable states, it is still informative to examine the behavior of the energy spectrum versus $k_f \gamma$, beginning with the breathing mode frequency. As the interaction strength becomes more negative Fig. 7 shows that the curvature about the local minimum in V_{eff} decreases. This “softening” of the hyperradial potential leads to a decrease in the breathing mode frequency in the outer well. Fig. 11 shows the breathing mode vs. $k_f \gamma$ predicted by the K harmonic (curve) method

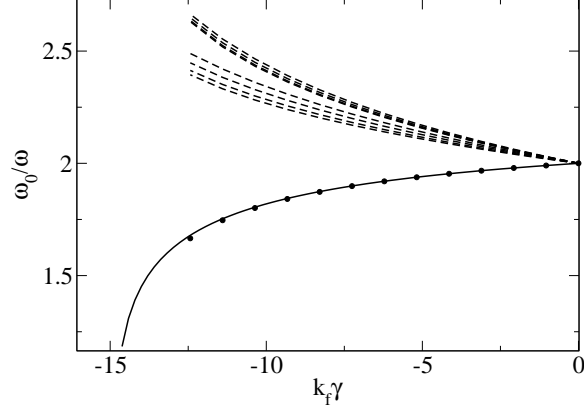


FIG. 11: The frequency of the lowest energy radial transition in units of the trap frequency versus $k_f\gamma$ predicted by the K harmonic method (solid line) and by the sum rule (circles). Also shown are the lowest eight radial transitions predicted by Hartree-Fock.

and also using the sum rule with Hartree-Fock orbitals (circles). Also shown in Fig. 11 are the lowest eight Hartree-Fock excitation frequencies for a filled shell of 240 atoms. Again, the K harmonic method agrees quite well with the sum rule, while both differ qualitatively from the HF prediction. The sharp decrease in the breathing mode frequency that occurs as $k_f\gamma \rightarrow k_f\gamma_c$ is a result of the excited mode “falling” over the barrier into the collapse region as the barrier is pulled down by the interaction. Figure 12 displays some energy levels in the metastable region as functions of $k_f\gamma$ near $k_f\gamma_c$. Because of the singular nature of the $1/R^3$ behavior in the inner region we have added an inner repulsive $1/R^{12}$ barrier to truncate the infinitely many nodes of the wavefunction in the inner region. The behavior of the wavefunction is not correct within this region anyway because recombination would become dominant, and in any case the zero-range interaction is suspect beyond $|k_f a| \sim 1$ and it must be renormalized. Figure 12 shows three distinct types of energy level. Levels that are contained in the local minimum (shown in blue) are decreasing, but not as quickly as the others; levels that are in the collapse region (shown in red) have a very steep slope as they are drawn further into toward $R = 0$; and energy levels that are above the barrier in V_{eff} (shown in purple) have wavefunctions are in both the collapse region and the local minimum. As $k_f\gamma$ decreases, the higher energy levels fall over the barrier into the collapse region earlier, until finally just before $k_f\gamma_c$ is reached the lowest metastable level falls below the “ground state”. This corresponds to the breathing mode behavior seen in Fig. 11. Of course all

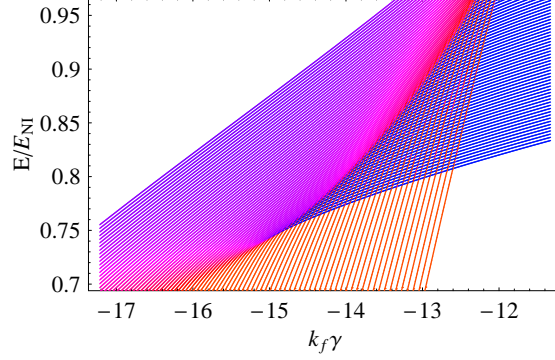


FIG. 12: (color online) A portion of the energy spectrum vs $k_f\gamma$ close to the critical point $k_f\gamma = k_f\gamma_c$. Levels in the metastable region (blue) decrease slowly while levels in the collapse region (red) decrease very quickly. Energy levels above the barrier in V_{eff}^s (purple) live both in the collapse region and the metastable region.

of this applies only if there is no further hyperradial dependence of g . If the interaction becomes density dependent, as is the case in some types of renormalization, a change in the hyperradius will change the density and thus the interaction coupling parameter, i.e. $g \rightarrow g(R)$.

C. The large N limit

In Sections IIIa and IIIb the ground state energy and expectation values discussed were found by solving the hyperradial effective Schrödinger equation 3.7 for a finite number of particles. Here we discuss the behavior of the N fermion system in the limit where N is large. To do this we exploit the fact that the $\partial^2/\partial R^2$ term in the effective Hamiltonian, the “hyperradial kinetic energy”, becomes negligible. In this limit we see that the total energy of the system is merely given by $E = V_{eff}(R_{\min})$, as is the case in dimensional perturbation theory.[23] To find the ground state energy we must merely find the minimum (local minimum for $g < 0$) value of V_{eff} . Accordingly, we find the roots of $\frac{dV_{eff}}{dR'} = 0$. Using Eq. 3.11 we simplify this to

$$k_f\gamma = \frac{1}{3\sigma} R'_{\min} (R'^4_{\min} - 1) \quad (3.16)$$

where R'_{\min} is the hyperradial value that minimizes V_{eff} . The solutions to Eq. 3.16 are illustrated graphically in Fig. 13; for any given $k_f\gamma$ we need only look for the value of R'_{\min}

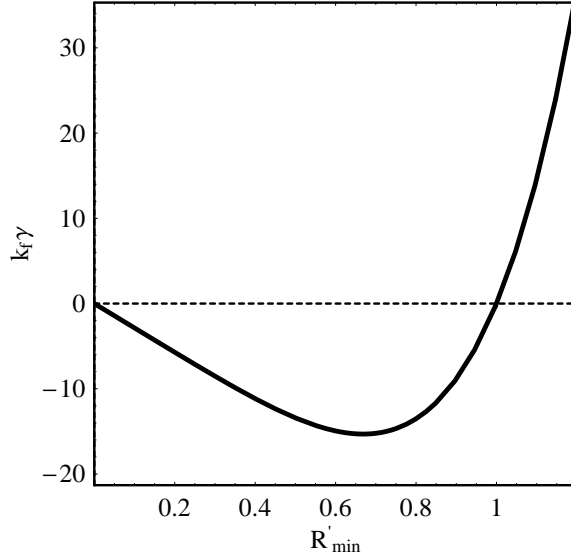


FIG. 13: Plot of the potential curve extrema which obey (3.16). Examination of this plot tells us the behavior of R'_{\min} for all allowed values of $k_f\gamma$ including the existence of the critical point $k_f\gamma_c$ located at the minimum of the plot where the maximum and minimum coincide.

that gives that value. The exact solution of Eq. 3.16 cannot be determined analytically for all values of $k_f\gamma$, but Fig. 13 shows that for $k_f\gamma > 0$ there is always only one positive, real R'_{\min} that satisfies Eq. 3.16. This corresponds to the global minimum discussed for repulsive interactions. For $k_f\gamma < 0$ things are a bit more complicated. Fig. 13 shows that for $k_f\gamma_c < k_f\gamma < 0$ there are two solutions to 3.16. The inner solution is a local maximum and corresponds to the peak of the barrier seen in Fig. 7, the outer solution corresponds to the local minimum where the DFG lives. The local minimum is the state that we are concerned with here as this will give the energy and hyperradial expectation values of the metastable Fermi gas. The value of $k_f\gamma$ where these two branches merge is the place where the local maximum merges with the local minimum namely the critical value $k_f\gamma_c$. Any value of $k_f\gamma$ less than $k_f\gamma_c$ has no solution to 3.16 and thus we cannot say that there is a region of stability. For $k_f\gamma = 0$, the non-interacting limit, we see that there are two solutions $R'_{\min} = 0$ and $R'_{\min} = 1$. The solution $R'_{\min} = 0$ must be discounted as there is a singularity in V_{eff} at $R = 0$. Thus in the non-interacting limit $R'_{\min} \rightarrow 1$ and $V_{eff}(R_{\min}) \rightarrow E_{NI}$, as expected.

Substitution of 3.16 into 3.11 gives the energy of the ground state in the large N limit,

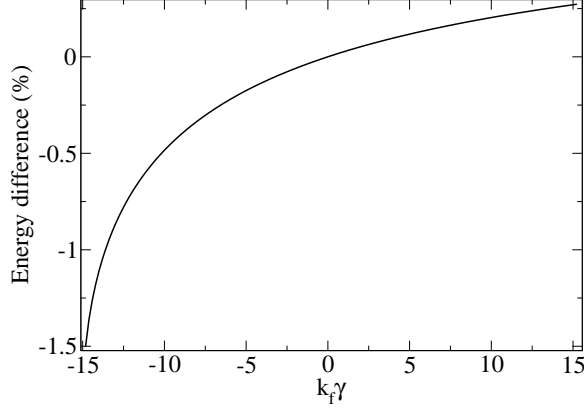


FIG. 14: The percentage difference between the energy found by minimizing V_{eff} and the energy found by explicitly solving the hyperradial Schrödinger equation for 240 atoms.

as a function of the size of the gas.

$$\frac{V_{eff}(R_{\min})}{E_{NI}} = \frac{1 + 5R_{\min}^4}{6R_{\min}^2}.$$

These solutions to Eq. 3.16 immediately give the ground state energy of the gas versus $k_f\gamma$. Fig. 14 shows the percentage difference of the ground state energy found by this minimization procedure and that of 240 particles found by diagonalizing H_{eff} in Eq. 3.7. We see in Fig. 14 that for $|k_f\gamma| < 10$ the energy difference is less than 0.5%. As $|k_f\gamma|$ gets larger the difference increases, but in the range shown the difference is always less than $\pm 1.5\%$.

Another result from 3.10 is the fact that in the large N limit the commutator $[H_{eff}, R] \rightarrow 0$. Thus for any operator that is solely a function of the hyperradius $\hat{O}(R)$ the ground state expectation value in the large N limit is given by the operator evaluated at R'_{\min} , i.e. $\langle \hat{O}(R') \rangle = \hat{O}(R'_{\min})$. This tells us that the large N limit wavefunction is given by $[R^{(3N-1)/2}G(R)]^2 = \delta(R - R_{\min})$. We can perturb this slightly and say that the ground state hyperradial wavefunction can be approximated by a very narrow Gaussian centered at R_{\min} . To find the width of this gaussian we approximate V_{eff} about R_{\min} as a harmonic oscillator with mass m^* and frequency ω_0 . We may find ω_0 by comparing the oscillator potential with the second order Taylor series about R_{\min} in V_{eff} , i.e.

$$\omega_0 = \sqrt{\frac{1}{m^*} \frac{1}{E_{NI}} \left(\frac{\partial^2 V_{eff}}{\partial R'^2} \Big|_{R'=R'_{\min}} \right)}. \quad (3.17)$$

The effective hyperradial oscillator length of $R^{(3N-1)/2}G(R)$ is then given by $l_0 = \sqrt{\hbar/m^*\omega_0}$.

The breathing mode frequency is now simply found to be ω_0 . The frequency in Eq. 3.17 is in units of the non-interacting energy, so to get back to conventional units we multiply by E_{NI}/\hbar . From Eq. 3.10 we know that $m^* = mE_{NI}N \langle R^2 \rangle_{NI}/\hbar^2$. Noting that $N \langle R^2 \rangle_{NI} = l^2 E_{NI}/\hbar\omega$ this leads to

$$\omega_0^B = \sqrt{\frac{1}{E_{NI}} \left(\frac{\partial^2 V_{eff}}{\partial R'^2} \Big|_{R'=R'_{min}} \right)}. \quad (3.18)$$

for ω_0^B , the breathing mode frequency in units of the trap frequency. Using Eq. 3.11 and substituting in Eq. 3.16 to evaluate at the minimum gives that

$$\omega_0^B = \sqrt{5 - \frac{1}{R'_{min}{}^4}}.$$

We note that this is now dependent only on the value of $k_f\gamma$, i.e. for a fixed $k_f\gamma$ the predicted breathing mode is independent of the number of atoms in the system in the large N limit.

This prediction can be compared with that predicted by the sum rule using the formula found by the authors of Ref. [22]:

$$\omega_0^B = \sqrt{4 + \frac{3 E_{int}}{2 E_{ho}}}. \quad (3.19)$$

Here E_{int} and E_{ho} are the expectation values of the interaction potential and the oscillator potential in the ground state respectively. If we insert the expectation values predicted here by the K harmonic method we find

$$\omega_0^B = \sqrt{4 + 3 \frac{\sigma k_f \gamma}{R'_{min}{}^5}}.$$

Substituting 3.16 for $k_f\gamma$ gives

$$\omega_0^B = \sqrt{5 - \frac{1}{R'_{min}{}^4}}$$

which agrees exactly with the frequency predicted in Eq. 3.19. Fig. 15 shows the breathing mode frequency predicted by Eq. 3.19 versus $k_f\gamma$. We see the same behavior in this plot as was seen in Fig. 11 where the breathing mode frequency dives to zero as $k_f\gamma \rightarrow k_f\gamma_c$.

IV. SUMMARY AND PROSPECTS

We have demonstrated an alternative approach to describing the physics of a trapped degenerate Fermi gas from the point of view of an ordinary linear Schrödinger equation

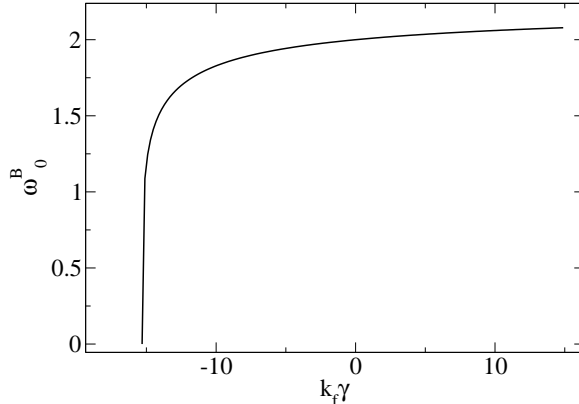


FIG. 15: The breathing mode (in oscillator units) in the large N limit versus $k_f \gamma$. Note that as $k_f \gamma \rightarrow k_f \gamma_c$ the frequency drops to zero as the local minimum disappears.

with two body, microscopic interactions. The use of a hyperspherical variational trial wave function whose hyperangular behavior is frozen to be that of the K harmonic yields a one-dimensional effective potential (3.8) in a collective coordinate, the hyperradius R . This approach yields an intuitive understanding of the energy and size of the DFG in terms of familiar Schrödinger quantum mechanics. Perhaps surprisingly, this approximation gives good results for the ground state energy, rms radius and peak number density of the gas. These are all in quantitative agreement with HF, while the breathing mode frequency compares well with that found using the sum rule method, but gives a qualitative improvement over the lowest calculated HF radial excitation frequencies.

The work presented here has been limited to the case of filled energy shells, i.e. “magic numbers” of atoms, and it should be readably generalizable, with minor extensions, to open shells as well. The present results are limited to a spherically symmetric trap. Generalization to an cylindrically symmetric “cigar” trap should be possible with a judicious choice of coordinates, and will be presented elsewhere.

For strongly attractive interactions, this picture predicts an instability in the DFG in a manner qualitatively similar to the physics of the “Bosenova”. [7] For the gas to remain stable across the BEC-BCS crossover regime the strength of interaction potential must be bounded from below, $k_f \gamma > -15.31$. Preliminary results from another study [24] indicate that renormalization of the singular δ -function interaction accomplishes precisely that, and apparently prevents collapse. The full interrelation between this picture and that of pairing

in the BEC-BCS crossover region is beyond the scope of this study and is a subject that will be relegated to future publications.

V. ACKNOWLEDGMENTS

This work was supported by funding from the National Science Foundation. We thank N. Barnea for introducing us to refs. [18, 19]. Discussions with L. Radzihovsky and V. Gurarie have also been informative.

APPENDIX A: HYPERRADIAL SOLUTION TO THE NON-INTERACTING OSCILLATOR

We wish to derive Eq. 2.15, the nodeless hyperradial solution to the Schrödinger equation for N non-interacting particles in an isotropic oscillator. The Schrödinger equation for this system is given by

$$\left[\sum_{i=1}^N \left(\frac{-\hbar^2}{2m} \nabla_i^2 + \frac{1}{2} m \omega^2 r_i^2 \right) - E \right] \Psi = 0 \quad (\text{A1})$$

where $\vec{r}_1, \vec{r}_2, \dots, \vec{r}_N$ are the cartesian coordinates for each atom from the trap center.

To begin we examine the radial Schrödinger equation for a single particle in an isotropic trap

$$\left(\frac{-\hbar^2}{2m} \left(\frac{d^2}{dr^2} - \frac{\ell(\ell+1)}{r^2} \right) + \frac{1}{2} m \omega^2 r^2 - E_{n\ell} \right) r f_{n\ell}(r) = 0. \quad (\text{A2})$$

The solution to this is well known and is given by

$$r f_{n\ell}(r) = A_{n\ell} \exp(-r^2/2l) \left(\frac{r}{l} \right)^{\ell+1} L_n^{\ell+1/2} \left(\frac{r^2}{l^2} \right) \quad (\text{A3})$$

with energy $E_{n\ell} = \hbar\omega(2n + \ell + 3/2)$ where $l = \sqrt{\hbar/m\omega}$ and n is the number of radial nodes in the wavefunction.

Transformation of (A1) into hyperspherical coordinates using Eqs. 2.2, 2.3, 2.5 and 2.7 yields a Schrödinger equation that separates into hyperradial and hyperangular pieces. The hyperangular solution is a hyperspherical harmonic that diagonalizes Λ^2 . The resulting hyperradial Schrödinger equation is given by

$$\left(\frac{-\hbar^2}{2R} \left(\frac{d^2}{dR^2} - \frac{K(K+1)}{R^2} \right) + \frac{1}{2} M \omega^2 R^2 - E \right) R^{(3N-1)/2} F(R) = 0. \quad (\text{A4})$$

where $K = \lambda + 3(N - 1)/2$. Comparing this with Eq. A2 we see that if we make the substitutions $\ell \rightarrow K$, $n \rightarrow \chi$, $m \rightarrow M$, $r \rightarrow R$ and $r f_{n\ell}(r) \rightarrow R^{(3N-1)/2} F_{\chi K}(R)$ the single particle radial Schrödinger equation becomes the N particle hyperradial Schrödinger equation. With these replacements the solution is evidently

$$R^{(3N-1)/2} G_{\chi K}(R) = A_{\chi K} \exp(-R^2/2\mathcal{L}) \left(\frac{R}{\mathcal{L}}\right)^{K+1} L_{\chi}^{K+1/2} \left(\frac{R^2}{\mathcal{L}^2}\right), \quad (\text{A5(a)})$$

where $\mathcal{L} = l/\sqrt{N}$ and χ is the number of hyperradial nodes in the N body system. For $\chi = 0$ this is the same hyperradial wavefunction written in Eq. 2.15. The total energy is given by

$$E_{\chi K} = \hbar\omega \left(2\chi + K + \frac{3}{2}\right) = \hbar\omega \left(2\chi + \lambda + \frac{3N}{2}\right) \quad (\text{A5(b)})$$

Now that we have a hyperspherical solution we can compare it with the solution to Eq. A1 written in terms of independent particle coordinates $(\vec{r}_1, \vec{r}_2, \dots, \vec{r}_N)$. This equation is clearly separable in each coordinate \vec{r}_i , and its solution is a product of N single particle wavefunctions

$$\Psi = \prod_{i=1}^N f_{n_i \ell_i}(r_i) y_{\ell_i m_i}(\omega_i)$$

Where $f_{n_i \ell_i}(r_i)$ is given by Eq. A3, ω_i are the spherical polar angular coordinates of the i th particle and $y_{\ell m}(\omega)$ is a normal 3D spherical harmonic. The energy for this independent particle solution is given by

$$E = \hbar\omega \left[\frac{3N}{2} + \sum_{i=1}^N (2n_i + \ell_i) \right]. \quad (\text{A6})$$

Now that we have seen that Eq. A1 is separable in both hyperspherical and independent particle coordinates, we may compare Eqs. A5(b) and A6 to find that

$$2\chi + \lambda = \sum_{i=1}^N (2n_i + \ell_i). \quad (\text{A7})$$

We should note that this does not mean that the independent particle solution and the hyperspherical solution are the exact same, only that the hyperspherical solution $F(R) \Phi_{\lambda}(\Omega)$ must be a linear combination of independent particle solutions of the same energy.

APPENDIX B: PROOF OF THEOREM 1

Here we will use the results from Appendix A to prove theorem 1. We proceed by assuming that there exists a fully antisymmetric, ground state, hyperspherical solution to

the Schrödinger equation for N non-interacting fermions in an isotropic trap with energy given by Eq. A5(b) with $\chi > 0$. If we can show that this leads to a contradiction then we have, from equation A7, that there is only one λ for all of the ground state configurations. From Appendix A we know that this hyperspherical solution must be a linear combination of antisymmetric, degenerate, ground state solutions in independent particle coordinates

$$F_{\chi K}(R) \Phi_{\lambda}(\Omega, \sigma_1, \sigma_2, \dots, \sigma_N) = \sum_{\nu} D_{\nu}(\vec{r}_1, \vec{r}_2, \dots, \vec{r}_N, \sigma_1, \sigma_2, \dots, \sigma_N)$$

where each D_{ν} is of the form of Eq. 2.13, ν is used to distinguish between degenerate states of the same energy and $F_{\chi K}(R)$ is given by Eq. A5(a). Again, for brevity, we suppress the spin coordinates $(\sigma_1, \sigma_2, \dots, \sigma_N)$ in Φ_{λ} . We now note that the hyperradius R is completely symmetric under all transpositions of particle coordinates, thus all of the transposition symmetry must be contained in the function $\Phi_{\lambda}(\Omega)$. From $\Phi_{\lambda}(\Omega)$ we construct a new completely antisymmetrized hyperspherical solution $F_{0K}(R) \Phi_{\lambda}(\Omega)$ which has energy

$$E = \hbar\omega \left(\lambda + \frac{3N}{2} \right).$$

Use of Eqs. A5(b) and A7 gives

$$\lambda = \frac{E_{NI}}{\hbar\omega} - \frac{3N}{2} - 2\chi, \quad (\text{B1})$$

where $E_{NI} = \hbar\omega \left[3N/2 + \sum_{i=1}^N (2n_i + \ell_i) \right]$ is the ground state energy as defined by any of the functions $D_{\nu}(\{\vec{r}_i\}_{i=1}^N)$. Thus our new function $F_{0K}(R) \Phi_{\lambda}(\Omega)$ has energy

$$E = E_{NI} - 2\chi$$

which would lie below the ground state energy, a contradiction unless $\chi = 0$.

In the above analysis we assumed a degenerate set of solutions at the ground state energy. For non-degenerate solutions the proof becomes trivial, as any nondegenerate solution must be the same no matter what coordinate system it is expressed in. From this the rest of the proof follows in the same way, and the final, unique λ for this system is given by Eq. B1,

$$\lambda = \frac{E_{NI}}{\hbar\omega} - \frac{3N}{2}. \quad (\text{B2})$$

APPENDIX C: CALCULATION OF THE S-WAVE INTERACTION MATRIX ELEMENT

To calculate C_N it is useful to start with a more general interaction. We assume that the interaction term in the total N body Hamiltonian is such that at a fixed hyperradius $U_{int}(\vec{r}_{ij})$ is separable into a hyperradial function times a hyperangular integral, i.e.

$$U_{int}(\vec{r}_{ij}) \equiv V_{ijR}(R) V_{ij\Omega}(\Omega). \quad (\text{C1})$$

From properties of the δ -function and Eq. 2.4 it is easy to see that the $U_{int}(\vec{r}) = g\delta^3(\vec{r})$ fits this criteria. While $V_{ij\Omega}(\Omega)$ might have some very complex form, it will be seen shortly that only the form of $V_{ijR}(R)$ and $U_{int}(\vec{r}_{ij})$ will matter.

$$U_{eff}(R) = \left\langle \Phi_\lambda \left| \sum_{i>j} U_{int}(\vec{r}_{ij}) \right| \Phi_\lambda \right\rangle$$

we may again use the antisymmetry of Φ_λ to exchange $\vec{r}_i \rightarrow \vec{r}_2$ and $\vec{r}_j \rightarrow \vec{r}_1$ and arrive at

$$U_{eff}(R) = \frac{N(N-1)}{2} \langle \Phi_\lambda | U_{int}(\vec{r}_{21}) | \Phi_\lambda \rangle.$$

From Eq. C1 we can write that

$$U_{eff}(R) = \zeta V_R(R) \quad (\text{C2})$$

Where $\zeta = \langle \Phi_\lambda | V_\Omega(\Omega) | \Phi_\lambda \rangle$ is the analogue of $gC_N/N^{3/2}$ in Eq. 3.5. To find ζ we may substitute in the definition $\Phi_\lambda(\Omega)$ from Eq. 2.16, multiplying by $R^{3N-1}G(R)^2$ on both sides, integrating over R and using Eq. C1 to replace $V_{21R}(R) V_{21\Omega}(\Omega)$ gives a simple equation that may be solve for ζ .

$$\zeta \alpha = \beta \quad (\text{C3(a)})$$

$$\alpha = \int R^{3N-1} G(R)^2 V_{21R}(R) dR \quad (\text{C3(b)})$$

$$\begin{aligned} \beta &= \frac{N(N-1)}{2} \int \prod_{j=1}^N d^3r_j D^* \left(\{\vec{r}_i\}_{i=1}^N \right) \\ &\quad \times U_{int}(\vec{r}_{21}) D \left(\{\vec{r}_i\}_{i=1}^N \right) \end{aligned} \quad (\text{C3(c)})$$

where $D \left(\{\vec{r}_i\}_{i=1}^N \right)$ is the Slater determinant defined in Eq. 2.13 and $G(R)$ is defined as in Eq. 2.15. We have also used that fact that $R^{3N-1}dRd\Omega = \prod_{j=1}^N d^3r_j$ [13]. ζ can now be found as a ratio of two integrals.

The integral, α , on the LHS of Eq. C3(a) can be calculated directly. The integral, β , on the RHS of Eq. C3(a) is now a diagonal, determinantal matrix element. β may be drastically simplified by using the orthogonality of the single particle basis functions (for details see [25], §6-1).

$$\begin{aligned} \beta = & \frac{1}{2} \sum_{i,j=1}^N \int d^3r_1 d^3r_2 \\ & \times \left[\psi_i^*(\vec{r}_1) \psi_j^*(\vec{r}_2) U_{int}(\vec{r}_{21}) \psi_i(\vec{r}_1) \psi_j(\vec{r}_2) \right. \\ & \left. - \delta_{m_{s_i} m_{s_j}} \psi_i^*(\vec{r}_2) \psi_j^*(\vec{r}_1) U_{int}(\vec{r}_{21}) \psi_i(\vec{r}_1) \psi_j(\vec{r}_2) \right] \end{aligned} \quad (\text{C4})$$

Where $\psi_i(\vec{r})$ is the i th single particle spatial wave function that appears in the product in Eq. 2.13, i.e.

$$r\psi_i(\vec{r}) = N_{n_i \ell_i} \exp(-r^2/2l^2) (r/l)^{\ell_i+1} L_{n_i}^{\ell_i+1/2} [(r/l)^2] y_{\ell_i m_i}(\omega). \quad (\text{C5})$$

With this result we can now specify to the s-wave interaction. Following Eq. C1 we may identify $U_{int}(\vec{r}_{21}) \longleftrightarrow g\delta^3(\vec{r}_{21})$ and $V_{21R}(R) \longleftrightarrow 1/R^3$. With this and Eq. 2.15, the integral in C3(b) is found to be

$$\alpha = \frac{\Gamma\left(\lambda + \frac{3(N-1)}{2}\right)}{\mathcal{L}^3 \Gamma\left(\lambda + \frac{3N}{2}\right)}. \quad (\text{C6})$$

Evaluating Eq. C4 begins by integrating the δ -function over \vec{r}_2 . This is simple and we can clearly see that the two terms in the integral in Eq. C4 have a common factor of $|\psi_i(\vec{r}_1)|^2 |\psi_j(\vec{r}_1)|^2$. Factoring this out gives

$$\beta = \frac{g}{2} \sum_{i,j=1}^N \left(1 - \delta_{m_{s_i} m_{s_j}}\right) \int d^3r_1 |\psi_i(\vec{r}_1)|^2 |\psi_j(\vec{r}_1)|^2. \quad (\text{C7})$$

This sum runs over all spatial and spin quantum numbers in a filled energy shell, we may break this up into to factors, a spin sum and a space sum

$$\begin{aligned} \beta = & \frac{g}{2} \sum_{m_{s_i}, m_{s_j} = -1/2}^{1/2} \left(1 - \delta_{m_{s_i} m_{s_j}}\right) \\ & \times \int d^3r_1 \left(\sum_{\nu} |\psi_{\nu}(\vec{r}_1)|^2\right) \left(\sum_{\mu} |\psi_{\mu}(\vec{r}_1)|^2\right) \\ = & g \int d^3r_1 \left(\sum_{\nu} |\psi_{\nu}(\vec{r}_1)|^2\right) \left(\sum_{\mu} |\psi_{\mu}(\vec{r}_1)|^2\right). \end{aligned} \quad (\text{C8})$$

where the Greek letters ν and μ stand for the set of spatial quantum numbers $\{n, \ell, m\}$. The spin sum is trivial and is given by $\sum_{m_{s_i}, m_{s_j}=-1/2}^{1/2} (1 - \delta_{m_{s_i} m_{s_j}}) = 2$. We may now calculate C_N for any given filled energy shell using Eq. C8 and plugging into the relationship

$$C_N = \frac{N^{3/2}}{g} \frac{\beta}{\alpha}. \quad (\text{C9})$$

This has been done for the first 100 filled shells the results of which are summarized by Fig. 1. C_N for a selection of shells is given in table I.

To extract C_N in the limit as $N \rightarrow \infty$ we may examine the expression for β in Eq. C8. We may note that the sum $\rho(\vec{r}) = \sum_{\nu} |\psi_{\nu}(\vec{r})|^2$ is the definition of the density of a spin polarized degenerate fermi gas of non-interacting particles in an isotropic oscillator. In the limit where $N \rightarrow \infty$ the trap energy of the non-interacting gas dominates the total energy. This means that the Thomas-Fermi approximation becomes exact in this limit. Thus we may write that

$$\rho(\vec{r}) = \frac{1}{6\pi^2} \left(\frac{2m\mu}{\hbar^2} \right)^{3/2} \left(1 - \frac{m\omega^2 r^2}{2\mu} \right)^{3/2} \quad (\text{C10(a)})$$

$$N_{m_s} = \int d^3r \rho(\vec{r}) \quad (\text{C10(b)})$$

The chemical potential μ may be found by the condition given in Eq. C10(b) where N_{m_s} is the number of particles with the same spin projection m_s . The system we are considering is an equal spin mixture so that $N_{\uparrow} = N_{\downarrow} = N/2$. Thus we find that $\mu = \hbar\omega (3N)^{1/3}$. Plugging this into Eq. C8 gives

$$\begin{aligned} \beta &= g \int [\rho(r)]^2 d^3r \\ &= g \sqrt{\frac{2}{3}} \frac{256}{315} \frac{N^{3/2}}{\pi^3 l^3}. \end{aligned} \quad (\text{C11})$$

We insert this into Eq. C9 with Eq. C6 to find that

$$C_N = \sqrt{\frac{2}{3}} \frac{256}{315\pi^3} N^{3/2} \frac{\Gamma\left(\lambda + \frac{3N}{2}\right)}{\Gamma\left(\lambda + \frac{3(N-1)}{2}\right)} \quad (\text{C12})$$

Using Eq. 3.4a for the large N behavior of λ , in the limit $N \rightarrow \infty$

$$C_N \longrightarrow \sqrt{\frac{2}{3}} \frac{32}{35\pi^3} N^{7/2} \quad (\text{C13})$$

which is the quoted large N behavior in Eq. 3.6.

It should be said that the same formalism that is presented in this paper can be applied to this system in center of mass coordinates. This is done by first choosing an appropriate set of Jacobi coordinates. $\vec{x}_i = \sqrt{i/(i+1)} \left(\sum_{j=1}^i \vec{r}_j/i - r_{i+1} \right)$ for $i = 1, \dots, N-1$ with the center of mass vector defined as $\vec{x}_{cm} = \sum_{j=1}^N \vec{r}_j/\sqrt{N}$. Hyperangular coordinates are now used to describe the $3N-3$ degrees of freedom in the Jacobi coordinates where $R^2 = \sum_{j=1}^{N-1} x_j^2/N = \left(\sum_{j=1}^N r_j^2 - x_{cm}^2 \right)/N$. The $3N-4$ hyperangles needed are now defined with respect to the lengths of the Jacobi vectors in the same way as in Eqs. 2.3 and 2.4. Under this coordinate transformation we find the Hamiltonian to be given by

$$H = H_{CM} + H_{R,\Omega}$$

Where H_{CM} is the hamiltonian for the center of mass coordinate \vec{x}_{cm} and $H_{R,\Omega}$ is an operator entirely defined by hyperspherical coordinates, i.e.

$$H_{CM} = \frac{-\hbar^2}{2m} \nabla_{cm}^2 + \frac{1}{2} m \omega^2 x_{cm}^2$$

$$H_{R,\Omega} = \frac{-\hbar^2}{2M} \left(\frac{1}{R^{3N-4}} \frac{\partial}{\partial R} R^{3N-4} \frac{\partial}{\partial R} - \frac{\Lambda^2}{R^2} \right) + \frac{1}{2} M \omega^2 R^2 + \sum_{i>j} U_{int}(\vec{r}_{ij})$$

With this Hamiltonian we make the ansatz that for $H\Psi = E\Psi$, $\Psi = \chi(\vec{x}_{cm}) G(R) \Phi_\lambda(\Omega)$ where χ is a wave function describing the center of mass motion, $G(R)$ is a nodeless hyperradial function and $\Phi_\lambda(\Omega)$ is the lowest hyperspherical harmonic in the $3N-4$ angular coordinates. We are then looking for the matrix element $\langle \Phi_\lambda | H_{R,\Omega} | \Phi_\lambda \rangle$ where the integral is taken over all hyperangles at fixed R . Theorem 1 still applies with the added idea that χ is given by the lowest s-wave state of the center of mass in an oscillator. From here the analysis presented in this section for trap centered coordinates still holds with the added change that the dimension of the hyperradial integral in Eq. C3(b) is three dimensions smaller. This leads to a factor in the interaction matrix element given by

$$C_N \rightarrow \frac{\left[\Gamma \left(\lambda + \frac{3(N-1)}{2} \right) \right]^2}{\Gamma \left(\lambda + \frac{3N}{2} \right) \Gamma \left(\lambda + \frac{3(N-2)}{2} \right)} C_N.$$

For smaller N this factor changes the interaction considerably, but for larger N it quickly goes to 1. Thus, in the large N from limit, besides extracting the center of mass “sloshing” modes, there is very little difference from the trap center coordinate systems in this Jacobi coordinate formalism.

VI. APPENDIX D: CALCULATING $\rho(0)$

We start from Eq. 3.14

$$\rho(0) = N \int dR R^{3N-1} |F(R)|^2 \int d\Omega \delta^3(\vec{r}_N) |\Phi_\lambda(\Omega)|^2.$$

If we can find $\int d\Omega \delta^3(\vec{r}_N) |\Phi_\lambda(\Omega)|^2$ then we have the solution. From Eq. 2.4 and properties of the δ -function we may say that

$$N \int d\Omega \delta^3(\vec{r}_N) |\Phi_\lambda(\Omega)|^2 = \frac{\xi}{R^3}.$$

We multiply this on both sides by the non-interacting hyperradial function $R^{3N-1} (G(R))^2$ and integrate over R .

$$N \int \int \delta^3(\vec{r}_N) |\Phi_\lambda(\Omega)|^2 (G(R))^2 R^{3N-1} dR d\Omega = \xi \int \frac{(G(R))^2}{R^3} R^{3N-1} dR \quad (\text{D1})$$

Inserting $G(R)$ from Eq. 2.15 to the right hand side is gives

$$\xi \int \frac{(G(R))^2}{N^{3/2} R^3} R^{3N-1} dR = \xi \frac{\Gamma[\lambda - 3(N-1)/2]}{\mathcal{L}^3 \Gamma[\lambda - 3N/2]}. \quad (\text{D2(a)})$$

From the definition of Φ_λ in Eq. 2.16 we see that the left hand side of D1 is a determinantal matrix element of a single particle operator integrated over all independent particle coordinates.

$$N \int \int \delta^3(\vec{r}_N) |\Phi_\lambda(\Omega)|^2 (G(R))^2 R^{3N-1} dR d\Omega = N \int \prod_{j=1}^N d^3 r \left| D(\{\vec{r}_i\}_{i=1}^N) \right|^2 \delta^3(\vec{r}_N) \quad (\text{D2(b)})$$

Where $D(\{\vec{r}_i\}_{i=1}^N)$ is the Slater determinant wave function defined in Eq. 2.13. Referring to the definition of the density ρ in Eq. 3.13 we see that this is merely the peak density of the non-interacting system $\rho_{NI}(0)$. Thus

$$\xi = \rho_{NI}(0) \frac{l^3 \Gamma[\lambda - 3N/2]}{N^{3/2} \Gamma[\lambda - 3(N-1)/2]}.$$

The peak density is then given by

$$\rho(0) = \xi \int dR \frac{R^{3N-1} |F(R)|^2}{R^3}$$

which is what we were seeking to show.

[1] M. Bartenstein, A. Altmeyer, S. Riedl, S. Jochim, C. Chin, J. H. Denschlag, and R. Grimm, Phys. Rev. Lett. **92**, 120401 (2004).

- [2] T. Bourdel, L. Khaykovich, J. Cubizolles, J. Zhang, F. Chevy, M. Teichmann, L. Tarruell, S. J. J. M. F. Kokkelmans, and C. Salomon, *Phys. Rev. Lett.* **93**, 50401 (2004).
- [3] J. Kinast, S. L. Hemmer, M. E. Gehm, A. Turlapov, and J. E. Thomas, *Physical Review Letters* **92**, 150402 (2004).
- [4] C. A. Regal, M. Greiner, and D. S. Jin, *Phys. Rev. Lett.* **92**, 40403 (2004).
- [5] M. W. Zwierlein, C. A. Stan, C. H. Schunck, S. M. F. Raupach, A. J. Kerman, and W. Ketterle, *Phys. Rev. Lett.* **92**, 120403 (2004).
- [6] S. T. Rittenhouse, M. J. Cavagnero, J. von Stecher, and C. H. Greene, *arXiv:cond-mat/0510454* (2005).
- [7] J. L. Bohn, B. D. Esry, and C. H. Greene, *Phys. Rev. A* **58**, 584 (1998).
- [8] Y. E. Kim and A. Zubarev, *J. Phys. B* **33**, 55 (2000).
- [9] D. Kushibe, M. Mutou, T. Morishita, S. Watanabe, and M. Matsuzawa, *Phys. Rev. A* **70**, 63617 (2004).
- [10] Y. F. Smirnov and K. V. Shitikova, *Sov. J. Part. Nucl.* **8**, 44 (1977).
- [11] D. Blume and C. H. Greene, *J. Chem. Phys.* **112**, 8053 (2000).
- [12] B. D. Esry, C. H. Greene, and J. P. Burke, *Phys. Rev. Lett.* **83**, 1751 (1999).
- [13] J. Avery, *Hyperspherical Harmonics: Applications in Quantum Theory* (Kluwer Academic Publishers, 1989).
- [14] N. Barnea, *J. Math. Phys.* **40**, 1011 (1999).
- [15] M. J. Cavagnero, *Phys. Rev. A* **33**, 2877 (1986).
- [16] M. Fabre de la Ripelle and J. Navarro, *Ann. Phys.* **123**, 185 (1978).
- [17] M. Fabre de la Ripelle, S. A. Sofianos, and R. M. Adam, *Ann. Phys.* **316**, 107 (2005).
- [18] N. K. Timofeyuk, *Phys. Rev. C* **65**, 064306 (2002).
- [19] N. K. Timofeyuk, *Phys. Rev. C* **69**, 034336 (2004).
- [20] E. Fermi, *Nuovo Cimento* **11**, 157 (1934).
- [21] B. D. Esry and C. H. Greene, *Phys. Rev. A* **60**, 1451 (1999).
- [22] L. Vichi and S. Stringari, *Phys. Rev. A* **60**, 4734 (1999).
- [23] T. C. Germann, D. R. Herschbach, M. Dunn, and D. K. Watson, *Phys. Rev. Lett.* **74**, 658 (1995).
- [24] B. M. Fregoso and G. Baym, *arXiv:cond-mat/0602191* (2006).
- [25] R. D. Cowan, *The Theory of Atomic Structure and Spectra* (University of California Press,

1981).